

RSC Advances



This is an *Accepted Manuscript*, which has been through the Royal Society of Chemistry peer review process and has been accepted for publication.

Accepted Manuscripts are published online shortly after acceptance, before technical editing, formatting and proof reading. Using this free service, authors can make their results available to the community, in citable form, before we publish the edited article. This *Accepted Manuscript* will be replaced by the edited, formatted and paginated article as soon as this is available.

You can find more information about *Accepted Manuscripts* in the [Information for Authors](#).

Please note that technical editing may introduce minor changes to the text and/or graphics, which may alter content. The journal's standard [Terms & Conditions](#) and the [Ethical guidelines](#) still apply. In no event shall the Royal Society of Chemistry be held responsible for any errors or omissions in this *Accepted Manuscript* or any consequences arising from the use of any information it contains.

1 Targeting Vitamin E TPGS-Cantharidin Conjugate Nanoparticles for Colorectal Cancer 2 Therapy

3 Shihou Sheng¹, Tao Zhang², Shijie Li³, Jun Wei⁴, Guangjun Xu⁴, Tianhong Sun⁵, Yahong Chen¹,

4 Fengqing Lu¹, Yongchao Li⁶, Jinghui Yang⁷, Huiqiu Yu⁸, Tongjun Liu^{1*}, Gang Han^{9**}

5 ¹Department of Colorectalrectal and Anal Surgery,China-Japan Union Hospital of Ji Lin
6 University,ChangChun 130000,China

7 ² Department of Gastrointestinal Surgery,China-Japan Union Hospital XinMin District of JiLin
8 University,ChangChun 130000,China

9 ³ Department of Thyroid Surgery,China-Japan Union Hospital of JiLin University,ChangChun
10 130000,China

11 ⁴Department of Neurosurgery, China-Japan Union Hospital of JiLin University, ChangChun 130000,China

12 ⁵ Department of Operating Room, China-Japan Union Hospital of JiLin University,ChangChun
13 130000,China

14 ⁶Department of Gastrointestinal Surgery, China-Japan Union Hospital of JiLin University, ChangChun
15 130000, China

16 ⁷Department of Hepatopancreatobiliary Surgery, China-Japan Union Hospital of JiLin University,
17 ChangChun, 130000,China

18 ⁸Department of Rehabilitation Medicine, China-Japan Union Hospital of JiLin University, ChangChun
19 130000,China

20 ⁹ Department of Gastrointestinal Surgery, The Second Hospital of JiLin University,ChangChun
21 130000,China

22 *corresponding author.Tel/fax:+86 431 89876792

23 **corresponding author.Tel:+86 18743099891

24

25

26

27 **Abstract:** A traditional Chinese medicine cantharidin which was previously found to be effective
28 on colorectal cancer cells was translated into nanoparticles for drug delivery to reduce its side effects and
29 enhance its drug efficacy. By further introducing the folate targeting ligands to the nanoparticles, targeting
30 delivery of cantharidin to colorectal cancer is realized. catharidin loaded nanoparticles can increase the
31 cytotoxicity of cantharidin on the folate over-expressed HT-29 cells; Moreover, introducing folate to the
32 nanoparticles can further increase its efficacy, while this obvious enhancement cannot be found on the
33 MCF-7 cells with lower folate receptors.

34

35 **Key words:** cantharidin, TPGS, nanoparticles, drug delivery, folate

36 **Introduction**

37 Nowadays, colorectal cancer has already become the third most commonly diagnosed cancer in
38 both men and women in US excluding skin cancer. Moreover, it is the second leading cause of death in
39 cancer patients in US for both men and women [1,2]. Though hundreds of potential anticancer drugs are
40 available on the market, most of them are not ideal, which can cause serious adverse effects [3]. A very
41 promising candidate is cantharidin, which is a type of terpenoid, a chemical compound secreted by many
42 species of blister beetle [4]. Cantharidin has long been used as a traditional Chinese medicine for the
43 treatment of a variety of cancers, including liver, lung, intestinal, and digestive tract tumors [4,5].
44 Researchers around the world have found that cantharidin as well as its derivatives demonstrated strong
45 affinity and specificity for protein phosphatase 2A (PP2A). It is reported that the level of PP2A inhibition
46 parallels their cytotoxicity [6]. Recently, cantharidin is also found to be effective against several colorectal
47 cancer cells through inhibition of heat shock protein and Bcl-2 associated athanogene domain 3
48 expressions by blocking heat shock factor 1 binding to promoters [7]. Nevertheless, cantharidin has
49 displayed serious side effects such as dysphasia, hematemesis, and dysuria [8]. Therefore, a potential
50 way of reducing the side effects but remain its activity is urgent.

51 Nanoparticle based drug delivery system (DDS), defined as DDS, with particle diameters of
52 approximately 100 nm or less, is attracting considerable attention worldwide as efficient cancer
53 therapeutics for overcoming some of the limitations of conventional anticancer drug therapy [9-10]. For an
54 efficient DDS, the right choice of a drug carrier is vital. A good example is d-alpha-tocopheryl
55 polyethylene glycol 1000 succinate monoester (TPGS), which is an amphiphilic PEGylated vitamin E and
56 can work as best surfactant for hydrophobic drugs both via encapsulating the drugs or conjugating with
57 the drugs and then assembling the conjugates into nanoparticulate drug delivery systems[11]. What's more,
58 the drug carrier TPGS has almost no toxic issues as it is widely applied in the food and drug industry [12].

59 Folate is a small molecular compound, which is very important for tumor cell proliferation and
60 survival. Several cancer cells were over-expressed folate receptors as much as 200-fold on the cell
61 surfaces compared to the normal cells. The over-expressed receptors are vital to the intake of folate to

62 the tumor cells [13,14]. Typically, folate receptor is over-expressed in ovarian cancer, breast cancer, head
63 and neck cancer, and some childhood cancers [15]. Given these attributes of folate receptors, folic acid
64 has been conjugated to many delivery systems for cancer therapy including liposomes, polymeric
65 micelles and capsules, upconversion nanoparticles and carbon nanotubes, etc [16-19]. Moreover,
66 previous study revealed that the folate receptor was highly expressed in colorectal cancers [20], which
67 makes it possible to utilize folate for target delivery of drugs for treatment of colorectal cancer.

68 Taking into account the unique anticancer property of cantharidin and the drug delivery
69 technology developed till far, researchers around the world have tried tremendous ways of delivering
70 cantharidin or its derivatives directly to the cancer cells for cancer therapy. Zhu, et al reported preparation
71 of cantharidin-loaded solid lipid nanoparticles (CA-SLNs) with oral bioavailability by a film dispersion–
72 ultrasonication method [21]. The result showed that CA-SLNs had a sustained release profile without a
73 burst effect and a higher bioavailability than free cantharidin after oral administration. Later, Zhu, et al
74 reported an inclusion complex of cantharidin with β -cyclodextrin for drug delivery [22]. However, the *in*
75 *vitro* and *in vivo* drug efficacy efficacy was not studied. More recently, norcantharidin, a demethyl
76 derivative of cantharidin with lower toxicity was conjugated to polyethylenimine (PEI) and polylysine (PLL)
77 for acid liable drug release by Shen, et al [23]. Though this system showed reasonable acid
78 responsiveness, the drug itself was not the more efficient cantharidin and the polymers used are not FDA
79 approved, making further clinical use harder. Taken together, we here show the first example of rational
80 design of cantharidin loaded TPGS nanoparticles for targeting delivery of cantharidin and effective
81 treatment of colorectal cancer. As cantharidin is an anhydride which can undergo readily reaction with
82 hydroxyl groups. Via a simple one step ring opening reaction of cantharidin with the end hydroxyl group of
83 TPGS, a cantharidin-TPGS conjugate (Can-TPGS, Scheme 1, a) was obtained. Due to the amphiphilic
84 nature of TPGS, this Can-TPGS conjugate can self-assemble in aqueous solution into nanoparticles as
85 effective cantharidin delivery systems (Scheme 1, b). To further increase the efficacy of this system, folate
86 was introduced to the nanoparticles via assembly of FA-TPGS and Can-TPGS together (Scheme 1,c).
87 The novel cantharidin loaded nanoparticles were systematically characterized and studied *in vitro* on two
88 cancer cell lines, HT-29 (human colorectal cancer cell, folate receptor over-expressed)[24] and MCF7
89 (Human breast cancer, folate receptor low-expressed)[25]. Results showed that catharidin loaded
90 nanoparticles can increase the cytotoxicity of cantharidin on the folate over-expressed HT-29 cells;
91 Moreover, introducing folate to the nanoparticles can further increase its efficacy, while this obvious
92 enhancement cannot be found on the MCF-7 cells.

93 **Materials**

94 4-dimethylaminopyridine (DMAP), folic acid, d-alpha-tocopheryl polyethylene glycol 1000
95 succinate monoester (TPGS) was purchased from Sigma-Aldrich. Cantharidin was purchased from Santa
96 Cruz Biotech. All other chemicals and reagents were used as reagent grade without further purification in
97 all of the experiments.

98 Instrumentation

99 ^1H NMR spectra were recorded at ambient temperature on a JEOL JNM LA400 NMR
100 spectrometer. The nanoparticles were analyzed using Transmission electron microscopy (TEM) (TEM;
101 JEOL JEM-1011). The Size and size distribution of the nanoparticles was then determined by dynamic
102 light scattering (DLS) with a vertically polarized He-Ne laser (DAWN EOS, Wyatt Technology, USA). The
103 scattering angle was fixed at 90° and the measurement was carried out at a constant temperature of 25°C .
104 The zeta potential of the nanoparticles prepared here was conducted on a Malvern Zetasizer Nano ZS
105 which was calibrated using a 60 nm polystyrene standard. Nanoparticle samples are prepared by
106 dissolving into de-ionized water and the particle size and zeta potential were measured simultaneously in
107 triplicate.

108 Synthesis of Can-TPGS conjugates

109 TPGS (1.5 g, 1 mmol) was dissolved in 50 mL anhydrous CH_2Cl_2 in a round flask, to which 1 N
110 cantharidin anhydride (0.196 g, 1 mmol) and DMAP (0.122 g, 1 mmol) were added. The reaction mixture
111 was heated to reflux under stirring overnight in an oil bath. After that, the reaction mixture was left cooled
112 down to room temperature and subjected to rotation evaporation. Then, the obtained product was
113 dissolved in 5 ml dimethylformamide (DMF) and subjected to 3 days of dialysis against water in a dialysis
114 bag with a molecular cut-off at 1000 Da. Then the purified product was collected and lyophilized as white
115 powder for further use.

116 Synthesis of FA-TPGS conjugates

117 TPGS (0.15 g, 0.1 mmol) was dissolved in 10 mL anhydrous dimethyl sulfoxide (DMSO) in a round
118 flask, to which 1 N folic acid (0.044 g, 0.1 mmol), DCC (0.041 g, 0.2 mmol) and DMAP (0.024 g, 0.2 mmol)
119 were added. The reaction mixture was kept in ice bath under stirring overnight. After that, the reaction
120 mixture was filtered to remove dicyclohexyl urea. Then the DMSO solution of the FA-TPGS conjugate
121 was put into a dialysis bag with a molecular cut-off at 1000 Da against DMSO for 3 days to remove
122 excess DCC and DMAP. In the meanwhile, DMSO outside the dialysis bag was changed several times.
123 After that, the product was dialyzed against water for 3 days. Then, it was collected and lyophilized to get
124 FA-TPGS powder.

125 Preparation of TPGS NPs and FA-TPGS NPs

126 For preparation of the blank carrier nanoparticles (TPGS NPs) and FA targeting blank
127 nanoparticles (FA-TPGS NPs), a nano-precipitation method was used [26]. Taking TPGS NPs as an
128 example, briefly, 20 mg of TPGS was dissolved in 2 ml of acetone under vigorously stirring, after that, 15
129 ml of de-ionized water was added. Then this solution was left stirring at room temperature for volatilizing
130 the acetone. Thereafter, the nanoparticles were lyophilized for further use. For making the targeting

131 nanoparticles, the starting materials become TPGS and FA-TPGS at a ratio of 0.95:0.05. All the other
132 steps were the same.

133 **Preparation of Can-NPs and FA-Can-NPs**

134 For preparation of the cantharidin loaded nanoparticles (Can-NPs) and folate targeting
135 nanoparticles (FA-Can-NPs), a nano-precipitation method was used [26]. Taking Can-NPs as an example,
136 briefly, 20 mg of Can-TPGS conjugates was dissolved in 2 ml of acetone under vigorously stirring, after
137 that, 15 ml of de-ionized water was added. Then this solution was left stirring at room temperature for
138 volatilizing the acetone. Thereafter, the nanoparticles were lyophilized for further use. For making the
139 targeting nanoparticles, the starting materials become Can-TPGS and FA-TPGS at a ratio of 0.95:0.05. All
140 the other steps were the same.

141 **Preparation rhodamine B loaded nanoparticles of Can/RhB-NPs and FA-Can/RhB-NPs**

142 To prepare fluorescent molecule labeled nanoparticles for further *in vitro* study, rhodamine B(RhB)
143 labeled Can-NPs and FA-Can-NPs called Can/RhB-NPs and FA-Can/RhB-NPs were prepared
144 respectively using the method described above[26]. First, RhB-TPGS conjugate was prepared as
145 previously described for FA-TPGS conjugates. Then the RhB-TPGS conjugate was used together with
146 Can-TPGS or Can-TPGS as well as FA-TPGS to prepare Can/RhB-NPs and FA-Can/RhB-NPs
147 respectively.

148 **Cantharidin drug release and Zeta potential monitoring during drug release**

149 The hydrolysis of cantharidin from Can-NPs was monitored by ^1H NMR spectroscopy as
150 previously described [23]. Briefly, Can-NPs (200 mg) were dissolved in 20 ml PBS (pH=7.4, 10 mM) or
151 acetate buffered solution (pH=5.0, 10 mM). The samples were put into the dialysis bag at a molecular
152 cutoff at 1000 Da with shaking. At desirable time intervals, 2 ml of samples was removed from the dialysis
153 bag. The collected polymer was subjected to ultra-centrifugation and washed 3 times by water to remove
154 salt and then lyophilized. Their ^1H NMR spectra were recorded. The degree of hydrolysis was calculated
155 by comparing the peak at 4.7ppm (peak c in cantharidin in Figure 1a) with the peak at 3.65 ppm of PEG (-
156 $\text{CH}_2\text{-CH}_2\text{-O-}$) in TPGS.

157 To monitor the Zeta potential change in drug release process, 0.5 mL of samples at pH5.0 and
158 pH7.4 respectively were collected at desirable time points and diluted to 3 mL for Zeta potential
159 monitoring. The initial samples prepared at t=0 were set as controls.

160 **Cell culture conditions and cell lines**

161 The cancer cell lines HT-29 (human colon cancer, folate receptor over-expression) and MCF-7
162 (human breast cancer, folate receptor negative expression) were maintained in McCoy's 5a media and
163 Eagle's minimum essential medium respectively. L-929 cells (mouse fibroblast) were cultured in DMEM.
164 All the culture media were supplemented with 10% FBS (fetal bovine serum), 0.03% L-glutamine and 1%
165 penicillin/streptomycin in 5% CO₂ at 37°C in a 95% humidified atmosphere.

166 ***In vitro* cytotoxic evaluation via MTT (3-(4,5-dimethylthiazol-2-yl)-2,5-diphenyltetrazolium bromide)** 167 **assay**

168 HT-29, MCF-7 and L-929 cells were harvested in a logarithmic growth phase and seeded on a
169 96-well plate in 100 µL media at a density of 5000 cells/well and incubated overnight. All the drugs were
170 dissolved in culture media and subjected for use. The cells were treated in three ways separately: 1) for
171 testing the compatibility of the blank micelles, the cells were treated with TPGS NPs and FA-TPGS NPs
172 from 15.6 µg/mL to 500 µg/mL; 2) for testing drug loaded micelles, Can-NPs and FA-Can-NPs with a
173 cantharidin concentration from 0.097 µM to 50 µM were used to treat the cells; 3) for folate competing
174 experiments, the cells were pre-treated with 2 mM sodium folate for 4 h and then the culture media was
175 removed, washed by PBS and new culture media was added. After that, FA-Can-NPs with a final
176 cantharidin concentration from 0.097 µM to 50 µM were added to the plates. After treatment of drugs, the
177 cells were transferred to an incubator at 37 °C for further incubation. At the end of the incubation for 48 h
178 at 37 °C, 10 µL of MTT (3-(4,5-dimethylthiazol-2-yl)-2,5-diphenyltetrazolium bromide) stock solution (5
179 mg/ml) is added to each culture well and further incubated for 4 hours. 100 µL of acidified isopropyl
180 alcohol-sodium dodecyl sulfate (SDS) solution was added to each well and incubated for another 12 h.
181 After that, the plate was read by a micro-plate reader at a wavelength of 570 nm.

182 **Intracellular localization and uptake efficiency study**

183 HT-29 cells were seed onto a glass in 6-wells plate at a density of 1 X10⁵ cells/well in 2 ml culture
184 media overnight before use. Then cells were then treated with Can/RhB NPs and FA-Can/RhB NPs at an
185 equal RhB concentration of 2 µg/ml for 1 h. Then the cells were washed twice with cold PBS, and fixed
186 with 4% formaldehyde. Cell nucleus was stained by DAPI (2-(4-amidinophenyl)-6-indolecarbamide
187 dihydrochloride). Cells were then thoroughly washed by PBS for three times and observed using confocal
188 laser scanning microscope (CLSM, Olympus FV1000).

189 For flow cytometry study, HT-29 cells were seed onto a glass in 6-wells plate at a density of 2
190 X10⁵ cells/well in 2 ml culture media overnight before use. Then cells were treated with Can/RhB-NPs,
191 FA-Can/RhB-NPs at an equal RhB concentration of 5 µg/ml. For FA blocking study, the cells were
192 pretreated with 2 mM FA and washed 3 times by cold PBS and then treated with FA-Can/RhB-NPs. For
193 lower temperature controls, cells were treated with the same procedures but the plates were put at 4 °C
194 instead. For NaN₃ mediated inhibition of endocytosis, before treatment of the drugs, cells were
195 pretreated with 20 mM NaN₃ and washed for 3 times by cold PBS prior to use. Each sample was
196 analyzed on a BD FACSCalibur™ flow cytometer (BD Biosciences).

197 **PP2A inhibition assay**

198 A million of HT-29 cells were seeded in a 6-well plate and incubated with cantharidin, Can-NPs,
199 FA-Can-NPs at an equal cantharidin concentration of 10 μ M for 6 h. Then the cells were washed for
200 several times, the cytosolic contents were extracted for PP2A activity assay. The PP2A activity is the
201 percentage of residual PP2A activity compared with untreated control groups. PP2A inhibition adds PP2A
202 activity equals to 1.

203

204 **Results and Discussion**

205 **Synthesis of Can-TPGS conjugates**

206 Secreted by blister beetle, most notably by the “Spanish fly”[4], cantharidin works by inhibiting protein
207 phosphatases 1 and 2A (PP1, PP2A)[6]. It has been a long time for people to use blister beetle to treat
208 *Molluscum contagiosum* virus (MCV) infections and associated warts. Nowadays, cantharidin has also
209 shown potent anticancer activities on many types of human cancer cells [4,5].

210 Although cantharidin possesses potent anti-tumor properties, the clinical application of cantharidin is
211 limited till far due to severe side-effects and its highly toxic nature [8]. Therefore, to find a way to reduce
212 its severe side effects becomes urgent. Recently, drug delivery systems (DDS) using liposomes,
213 biodegradable polymers, inorganic nano-materials such as nanotubes, nanocrystals, etc , have drawn
214 particular audience in the scientific world because they have the ability to reduce systemic toxicity and
215 improve tumor-targeting efficiency of therapeutic agents such as drugs, antibodies, proteins, siRNA and
216 imaging agents [27-31]. For this specific reason, we show here to utilize the most widely accepted TPGS
217 as a drug carrier to prepare a Can-TPGS conjugate. To prove the successful synthesis of the Can-TPGS
218 conjugate, ¹HNMR spectra of cantharidin, TPGS and Can-TPGS were collected in Figure 1(a-c). As
219 shown in Figure 1(a), the typical chemical proton shifts of -CH₃ at 1.24 ppm, -O-CH-CH₂-CH₂-CH-O- at
220 1.79 ppm and -CH₂-CH-O- at 4.73 ppm were assigned. Figure 1(b) collects the ¹HNMR of TPGS. The
221 peak at 3.65 ppm could be assigned to the -CH₂- protons of PEO in TPGS. The lower peaks in the
222 aliphatic region belong to various moieties of vitamin E tails. Figure 1(c) collects the ¹HNMR of Can-TPGS.
223 There appears a peak in 4.7 ppm which is typical chemical shift of -CH₂-CH-O- in cantharidin. By
224 integrating the peak compared to the PEO in TPGS, we can calculate that there is about 0.9 cantharidin
225 per TPGS, which means ca. 90% of the TPGS is end capped with cantharidin and a drug content of 11.5%
226 weight by weight.

227

228 **Preparation and characterization of TPGS NPs and FA-TPGS NPs**

229 TPGS is an amphiphilic molecule which can self-assemble into micelles in aqueous solution itself
230 [11]. To introduce the targeting ligand folate to the micelles, TPGS and FA-TPGS were co-assembled.
231 The TPGS NPs and FA-TPGS NPs were characterized by DLS and zeta potential analyzer. As shown in
232 Table 1, the mean diameter of TPGS is 65.7 \pm 2.5 nm with a polydispersity index (PDI) of 0.125. TPGS
233 NPs showed a zeta potential of -22.1 \pm 1.5 mV. For the FA-TPGS NPs, the mean diameter is 72.4 \pm 1.9

234 nm with a PDI of 0.135. Zeta potential of FA-TPGS NPs was -29.2 ± 3.1 mV, slightly lower than that of
235 TPGS NPs.

236

237 **Preparation and characterization of Can-NPs and FA-Can-NPs**

238 Cantharidin is conjugated to TPGS to make a Can-TPGS conjugate which can be further
239 assembled into micelles. Due to the hydrophilic nature of the free carboxyl group in the cantharidin
240 molecule, it will stay with PEG as the outer layer and the vitamin E can form the hydrophobic inner core.
241 Similarly, the size and size distribution of Can-NPs and FA-Can-NPs were characterized by DLS. Data
242 were shown in Figure 2a and Figure 2b and Table 1. Can-NPs and FA-Can-NPs had a mean diameter of
243 114.7 ± 1.2 nm and 130.4 ± 3.2 nm with a poly-dispersity index of 0.104 and 0.216 respectively. FA-Can-
244 NPs had a slightly larger diameter possibly due to the introducing of folate ligands onto the surface. From
245 the TEM images, spherical structures of both Can-NPs and FA-Can-NPs can be found with diameters of
246 102.5 nm and 110.7 nm respectively (Figure 2c and Figure 2d). The zeta potential of Can-NPs and FA-
247 Can-NPs were -35.6 ± 2.4 mV and -28.4 ± 3.5 mV. The negative charge is considered beneficial for
248 blood circulation.

249

250 **Drug release profiles of cantharidin and zeta potential change**

251 In order to study the drug release profiles of cantharidin from Can-NPs and FA-Can-NPs, we simplify
252 to study only Can-NPs rather than both of Can-NPs and FA-Can-NPs on the assumption that FA could
253 not change the drug release behavior of cantharidin. Here, a dialysis method was utilized for the drug
254 release study and two pH values at pH5.0 and pH7.4 for the dialysis buffer solution were chosen to
255 simulate the drug release in blood and in the tumor cells respectively due to the extensive report that the
256 pH in the tumor cells is around 5.0, while it is 7.4 in the blood [23]. Due to release and liberation of the
257 drug molecule cantharidin into the buffered solution, most of the released cantharidin can go through the
258 dialysis bag. At desirable time points, we collected the polymer solution in the dialysis bag and washed
259 the polymer via ultracentrifugation to remove the salt and residual cantharidin released, and then the
260 nanoparticles were collected and lyophilized for ^1H NMR measurement. By simply integrating the peak of
261 cantharidin at 4.7 ppm as compared to 3.65 ppm of PEG in TPGS, we can calculate the drug release
262 percentage. In Figure 3a, results showed that cantharidin was released much faster at pH5.0 than at
263 pH7.4. To be more specific, it can be found that at 48 h, 19% cantharidin was released at pH7.4, while
264 this was 48 % at pH5.0. The drug release difference between the two pH values can be explained by the
265 possible hydrolysis of the linkage of the ester bond at two different pH values. The fact that cantharidin is
266 released much faster at pH5.0 is would be beneficial for drug delivery to cancer cells due to the acidic
267 environment in the cancer cells [32].

268

269 As cantharidin was linked to TPGS with a bare carboxyl group on the end, there are many carboxyl
270 groups on the surfaces of Can-TPGS NPs. Once more and more cantharidin molecules are released, less

271 and less carboxyl groups would be present at the surfaces of Can-TPGS NPs. Therefore, monitoring the
272 Zeta potential during the drug release process may give some additional information to the drug release
273 process. As shown in Figure 3b, the freshly prepared Can-TPGS NPs at pH5.0 and pH7.4 had a zeta
274 potential of -25.3 mV and -39.6 mV respectively. The difference at the initial stage can be attributed to the
275 pH dependence of Zeta potential. At lower pH values (pH5.0), less carboxyl groups can be de-protonated,
276 therefore higher zeta potential could be found (-25.3 mV at pH5.0 vs -39.6 mV at pH7.4). As the
277 incubation time was prolonged, the drugs with carboxyl group were liberated from the surface of the
278 nanoparticles, the zeta potential became higher and higher both at pH5.0 and pH7.4. However, at pH5.0,
279 the Zeta potential increased much greater than that that at pH7.4, indicating more drugs were released at
280 5.0.

281

282 ***In vitro* evaluation of TPGS NPs and FA-TPGS NPs**

283 TPGS is widely used in pharmaceutical applications. TPGS has shown proven properties to improve
284 bioavailability of poorly absorbed drugs. As a water soluble compound, TPGS is also used as an efficient
285 source of natural vitamin E both for therapeutic purposes and nutrition. To prove that TPGS NPs and FA-
286 TPGS NPs are non-toxic to the two cancer cell lines HT-29 and MCF-7, TPGS NPs and FA-TPGS NPs
287 were treated with the cells for 48 h at a concentration ranging from 500 µg/ml to 16.25 µg/ml. As shown in
288 Figure 4a and Figure 4b, we can find that even up to 500 µg/ml, the cell viability for the two cell lines are
289 larger than 90%. And it can be further found that HT-29 and MCF-7 cells displayed no difference in cell
290 viability on the two kinds of nanoparticles, TPGS NPs and FA-TPGS NPs. This can be explained by the
291 fact that the two nanoparticles had no drugs and cells cannot be killed though there is possible targeting
292 effect. From the above results, we can find that TPGS NPs and FA-TPGS NPs are safe enough as drug
293 carriers.

294

295 ***In vitro* evaluation of Can-NPs and FA-Can-NPs**

296 The anti-cancer therapeutic promise of cantharidin is limited because of its high mammalian toxicity
297 [8]. Recent study has shown that cantharidin displayed considerable toxicity on some colorectal cancer
298 cell lines [7]. To reduce the side effects and further possibly increase the efficacy of cantharidin, here we
299 prepared a Can-TPGS conjugate and self-assembled this conjugate into nanoparticles to deliver
300 cantharidin to the cancer cells. In this way, we believe that the Can-NPs can release the drug cantharidin
301 to kill the cancer cells. Further by targeting the cells with folate ligand, the efficacy of FA-Can-NPs would
302 be higher than that of Can-NPs. To test the targeting effect of folate ligand, here we choose a colorectal
303 cancer cell line, HT-29 and a breast cancer cell line MCF-7 because the former one is reported to have
304 over-expressed folate receptors while the latter one has low-expressed folate receptors [24,25]. Moreover,
305 pretreatment of the cells with 2 mM folate was utilized to block the folate receptors. The results of Can-
306 NPs and FA-Can-NPs on two cell lines were shown as in Figure 5a and Figure 5b. In Figure 5a, it was
307 found that cantharidin showed a dose dependent cytotoxicity towards HT-29 cells at a concentration

308 ranging from 0.097 μM to 50 μM to (2-fold dilution). Can-NPs were much more effective than cantharidin
309 almost in all the concentration range. For the targeting nanoparticles, FA-Can-NPs, the cytotoxicity is
310 increased to a greater extent. Pretreatment of the cells with 2 mM folate to block the folate receptors on
311 the cell surfaces can reduce the efficacy of FA-Can-NPs. In this situation, the efficacy of FA-Can-NPs is
312 somewhat the same as non-targeting nanoparticles Can-NPs. The results here demonstrated that the
313 efficacy of the drugs are in the order of FA-Can-NPs > Can-NPs \approx FA-Can-NPs + FA > cantharidin on
314 HT-29 cells. This can be possibly explained by the targeting effect of the folate ligands and the delivery of
315 drugs to the cancer cells.

316 To further prove that, MCF-7 cells with low-expression of folate receptors was tested and the results
317 were shown in Figure 5 b. We can find that the efficacy of the drugs was in the order of FA-Can-NPs \approx
318 FA-Can-NPs + FA \approx Can-NPs > cantharidin. The results mean that folate targeting ligand has minimum
319 targeting effect on the folate receptor low-expressed cells. However, all the nanoparticles are better than
320 the free drug cantharidin, this is possibly due to the intracellular delivery of more drugs to the cells via the
321 nanoparticles.

322 To make it clearer, the IC_{50} values of cantharidin, Can-NPs, FA-Can-NPs and FA-Can-NPs blocked
323 by free FA on HT-29 and MCF-7 cells at 48 h were listed in Figure 5c and Figure 5d. As shown in Figure
324 5c, the IC_{50} values for cantharidin, Can-NPs and FA-Can-NPs and FA-Can-NPs+ FA (blocked by 2 mM
325 folate) were 15.3, 9.2, 3.6 and 8 μM on HT-29 cells at 48 h. Delivery of cantharidin by nanoparticles (Can-
326 NPs) can increase the efficacy of cantharidin by ca. 1.7 fold. Further targeting the nanoparticles can
327 increase its efficacy up to approximately 4.3 fold. Therefore, the extra 2.5 fold increase in efficacy can be
328 attributed to the targeting effect of folate. Further, we can take a look at the MCF-7 cell line as shown in
329 Figure 5d. The IC_{50} values for cantharidin, Can-NPs and FA-Can-NPs and FA-Can-NPs+ FA (blocked by
330 2 mM folate) were 32.4, 16.5, 13.1 and 14.7 μM respectively at 48 h. One can clearly find that delivery of
331 cantharidin by nanoparticles (Can-NPs) can increase the efficacy of cantharidin by ca. 1.9 fold. However,
332 further targeting the nanoparticles did not show any obvious increase in its efficacy and blocking the cells
333 with 2 mM folate also demonstrated no effect on the enhancement of drug efficacy. This is possibly due to
334 the low-expression of folate receptors on MCF-7 cells.

335 Moreover, to further show the benefit of delivery cantharidin, we have chosen a mouse fibroblast
336 cells to test the toxicity of cantharidin and Can-NPs. The results were shown in Fig.5e. We can clearly see
337 that both cantharidin and Can-NPs showed less toxicity on this cell lines than on MCF-7 and HT-20 at the
338 same doses, indicating the preference to kill the cancer cells by the Can-NPs.

339 Intracellular uptake of Can-NPs and FA-Can-NPs

340 To give some insight into the intracellular uptake of Can-NPs and FA-Can-NPs, first the cells
341 were treated with RhB loaded micelles Can/RhB-NPs and FA-Can/RhB-NPs at an equal RhB
342 concentration of 2 $\mu\text{g}/\text{ml}$. After treatment of them for 1 h, the cells were imaged via confocal laser

343 scanning microscope. The results were shown in Figure 6a. The blue fluorescence comes from DAPI in
344 the cell nucleus. The red fluorescence, which comes from RhB and stands for the nanoparticles, diffused
345 into the whole cells and mainly in the cytosol, indicating that Can-NPs entered the cancer cells. It should
346 be noted that at the same 1 h, cells treated with FA-Can-NPs displayed brighter red fluorescence,
347 suggesting more FA-Can/RhB-NPs were in the cells and existence of possible FA targeting of the cancer
348 cells.

349 Free anticancer drugs such as doxorubicin, paclitaxel, cisplatin as well as cantharidin are widely
350 believed to enter the cancer cells via passive diffusion [33]. However, the nanoparticles are extensively
351 reported to be internalized by the cancer cells via a different uptake pathway, via so-called endocytosis,
352 which is an energy dependent process. To explain why the nanoparticle formulation of cantharidin is
353 better than the free drug and FA-Can-NPs internalized more drugs than Can-NPs, here we studied
354 intracellular uptake of the drugs via flow cytometry. To track the nanoparticles in this process, we labeled
355 the Can-NPs and FA-Can-NPs with RhB (Can/RhB-NPs and FA-Can/RhB-NPs). Furthermore, to prove
356 the endocytosis of Can-NPs and FA-Can-NPs, 4 °C and 20 mM NaN₃ (ATP depleting agent) were used to
357 inhibit the energy dependent process [34]. As shown in Figure 6b, taking HT-29 as a representative
358 cancer cell line, we can found that FA-Can/RhB-NPs had more than 1.8-fold uptake of nanoparticles
359 compared to the non-targeting nanoparticles of Can/RhB-NPs (control). Blocking the cells with 2 mM
360 folate can greatly reduce the relative uptake of the Can/RhB-NPs to 1.1. The energy inhibition can greatly
361 affect the uptake as is can be seen from rapid reduction of the relative uptake values. It can be further
362 found that 4°C had shown a more profound effect on uptake than pretreatment of cells with 20 mM
363 NaN₃. The results above clearly revealed that Can/RhB-NPs were internalized by endocytosis and folate
364 targeting can increase the endocytosis efficiency of cantharidin loaded nanoparticles.

365

366 **PP2A inhibition assay**

367 It is generally believed cantharidin exert its anticancer efficacy via a strong affinity and specificity
368 for protein phosphatase 2A (PP2A)[6]. Moreover, scientist around the world have found that the level of
369 PP2A inhibition parallels its cytotoxicity for cantharidin[6]. To find whether Can-NPs and FA-Can-NPs
370 showed the same PP2A inhibition mechanism. A PP2A inhibition assay was studied on the HT-29 cells by
371 treatment of cantharidin, Can-NPs and FA-Can-NPs at 10 μM for 6 h. As shown in Figure 7, compared to
372 the non-treated cells (control), the PP2A activity of the cells treated with cantharidin, Can-NPs, FA-Can-
373 NPs, FA-Can-NPs + FA were 52 %, 41 %, 25% and 33% respectively. Therefore, the nanoparticles
374 loaded with cantharidin have shown PP2A inhibition efficacy. In accordance with the cell viability assay,
375 targeting cantharidin nanoparticles increase the inhibition of PP2A, while blocking the cells with 2 mM
376 folate will reduce the inhibition rate.

377

378 **Conclusion**

379 Taken together, we have shown here rational design of nanoparticles loaded with cantharidin via
380 a Can-TPGS conjugate for drug delivery. By further introducing the folate targeting ligand, we have
381 shown here folate targeting nanoparticles FA-Can-NPs loaded with cantharidin. The drug conjugate was
382 thoroughly characterized and two kinds of nanoparticles were systematically studied *in vitro*. We have
383 found that folate targeting nanoparticles with cantharidin to kill colorectal cancer via a PP2A dependent
384 way. Further *in vivo* evaluation of this system is on-going and this cantharidin loaded nanoparticles may
385 find the potential use in the future.

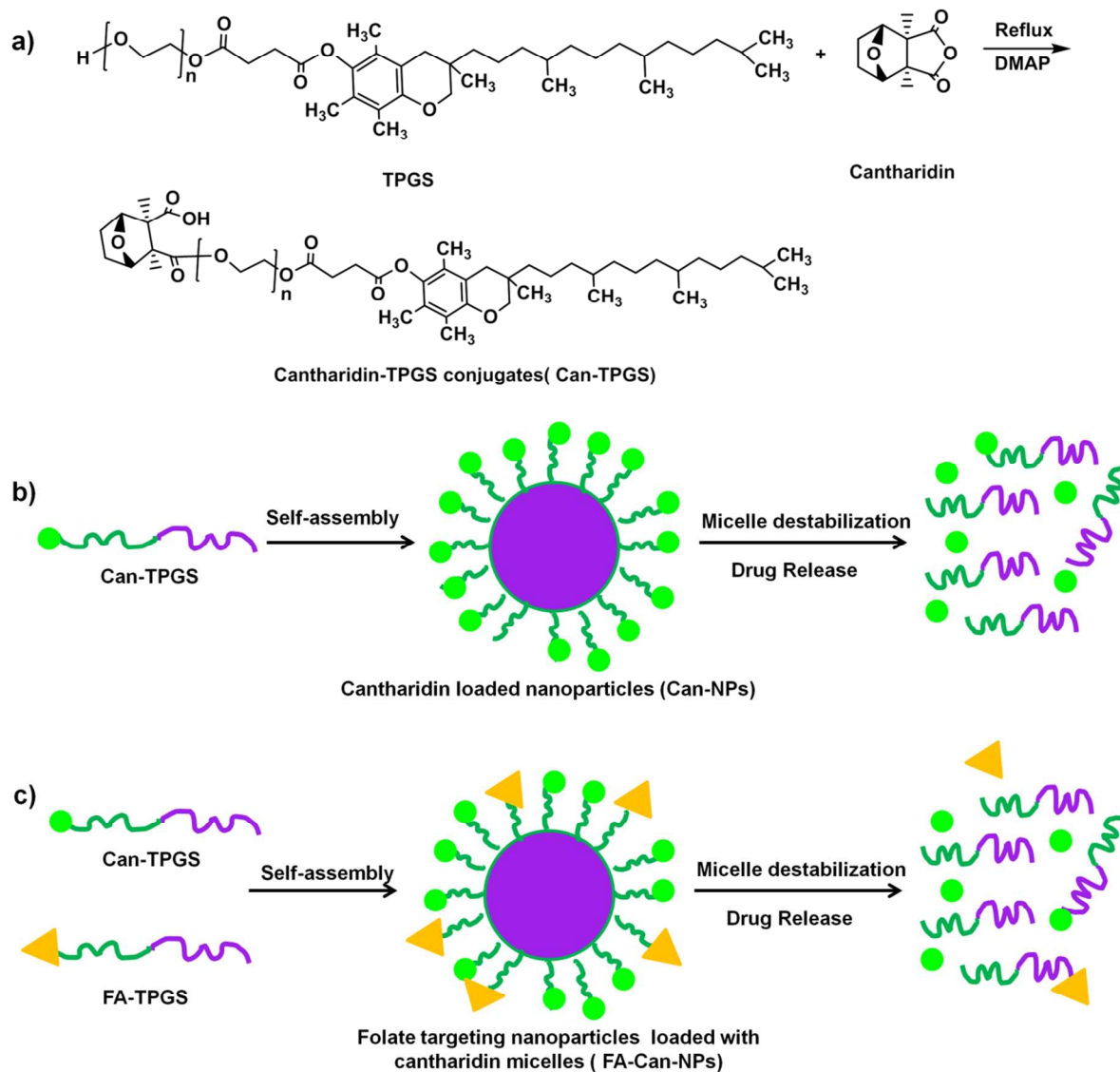
386

387

388 **References:**

- 389 [1] S. Rebecca, M. Kimberly, J. Ahmedin, CA Cancer J Clin, 65(2015) 5
390 [2] S. Rebecca, D. Carol, J. Ahmedin, CA Cancer J Clin, 64(2014) 104
391 [3] V. MacDonald, Can. Vet. J. 50 (2009) 665.
392 [4] E.P. Cherniack, Altern. Med. Rev. 15 (2010) 124.
393 [5] C.E.P. Puerto, L.Y.V. Méndez, V.V. Kouznetsov, Chem. Biol. Drug Des. 82 (2013) 477.
394 [6] O. Kadioglu, N.S. Kermani, G. Kelter, U. Schumacher, H.H. Fiebig, H.J. Greten, et al., Biochem.
395 Pharmacol. 1 (2014) 399.
396 [7] J.A. Kim, Y. Kim., B.M. Kwon, D.C. Han., J. Biol Chem.288 (2014)28713.
397 [8] G.S. Wang, J. Ethnopharmacol. 26 (1989) 147.
398 [9] G. Tiwari, R. Tiwari, B. Sriwastawa, L. Bhati, S. Pandey, P. Pandey, et al., Int. J. Pharm. Investig. 2
399 (2012) 2.
400 [10] T.M. Allen, P.R. Cullis, Science 19 (2004) 1818.
401 [11] L. Mu, S.S Feng, J. Control. Release 80 (2002) 129.
402 [12] Z. Zhang, S. Tan, S.S. Feng, Biomaterials 33 (2012)4889.
403 [13] L.E. Kelemen, Int. J. Cancer 119 (2006) 243.
404 [14] Q.Q. Zhu, C. Feng, W.W. Liao, Y. Zhang, S.Q. Tang, Cancer Cell Int. 13 (2013) 65.
405 [15] G.L. Zwicke, G.A. Mansoori, C.J. Jeffery, Nano Rev. 3 (2012) 10.
406 [16] J. Sudimack, R.J. Lee, Adv. Drug Deliver. Rev. 41 (2000) 147.
407 [17] S. Wang, P.S. Low, J. Control. Release 53 (1998) 39.
408 [18] A. Gabizon¹, A.T. Horowitz, D. Goren, D. Tzemach, H. Shmeeda¹, S. Zalipsky, Clin. Cancer Res. 9
409 (2003) 6551.
410 [19] X.Q. Yang, S. Pill, J.J. Grailer, D.A. Steeber, S.Q. Gong, Y.H. Chen, et al., J. Mater. Chem. 19 (2009)
411 5812.
412 [20] M.D. Angelica, J. Ammori, M. Gonen, D.S. Klimstra, P.S. Low, L. Murphy, M.R. Weiser, P.B.
413 Paty,Fong, R.P. Dematteo, P. Allen, W.R. Jarnagin, J, Shia. Modern Pathology 24(2011)1221.
414 [21] Y.J. Dang, C.Y. Zhang, Chin. Med. 8(2013) 1

- 415 [22] Y.J.Dang, L. N. An, C.H. Hu, C. Y. Zhu, J. Appl. Polym. Sci. 123(2013)1557
- 416 [23] K.D. Lu, M.Z. Cao, W.W. Mao, X.R. Sun, J.B. Tang, Y.Q. Shen, M. H. Sui, J. Mater.Chem.
417 22(2012)15804
- 418 [24] M.D. Nonancourt-Dition, J.L. Gueant, C. Adjalla, C. Chery, R. Hatier, F. Namour. Cancer let.
419 171(2001)139.
- 420 [25] G.A. Mansoori, K.S. Brandenburg. Cancers 2(2010) 1911
- 421 [26] D. Lin, G. Li, L. Qin, Z. Wen, J. Wang, X. Sun. J Biomed. Nanotechnol. 9 (2013) 2017.
- 422 [27] K.P. Singh, P. Preety, K. Pooja, Sanjesh, J. Biomed. Nanotechnol. 7 (2011) 60.
- 423 [28] L. Zhang, F.X. Gu, J.M. Chan, A.Z. Wang, R.S. Langer, O.C. Farokhzad, Clin. Pharmacol. Ther. 83
424 (2008) 761.
- 425 [29] Y. Wen, W.S. Meng, J. Pharm. Innov. 9 (2014)158
- 426 [30] Y. Wen, H.R. Kolonich, K.M. Kruszewski, N. Giannoukakis, E.S. Gawalt, W.S. Meng, Mol. Pharm. 10
427 (2013) 1035
- 428 [31] A. Balducci, Y. Wen, Y. Zhang, B.M. Helfer, T.K. Hitchens, W.S. Meng, A.K. Wesa, J.M. Janjic.
429 Oncoimmunology 2 (2013) e23034
- 430 [32] S.F. Yua, G.L. Wua, X. Gua, J.J. Wang, Y.N. Wang, H. Gao, et al., Colloid. Surface. B. 103 (2013)
431 15.
- 432 [33] M.J. Ratain, W.K. Plunkett, Holland-Frei Cancer Medicine. 6th edition, 2003.
- 433 [34] S. Vranic, N. Boggetto, V. Contremoulins, S. Mornet, N. Reinhardt, F. Marano, et al., Part. Fibre
434 Toxicol. 10 (2013) 2.



Scheme 1. Preparation of the folate targeted nanoparticles loaded with cantharidin. (a) Synthesis of the cantharidin TPGS conjugates (Can-TPGS); (b) Self-assembly of the Can-TPGS conjugates to cantharidin loaded nanoparticles (Can-NPs); (c) Self-assembly of the Can-TPGS conjugates with folate-TPGS (FA-TPGS) to folate targeting nanoparticles (FA-Can-NPs).

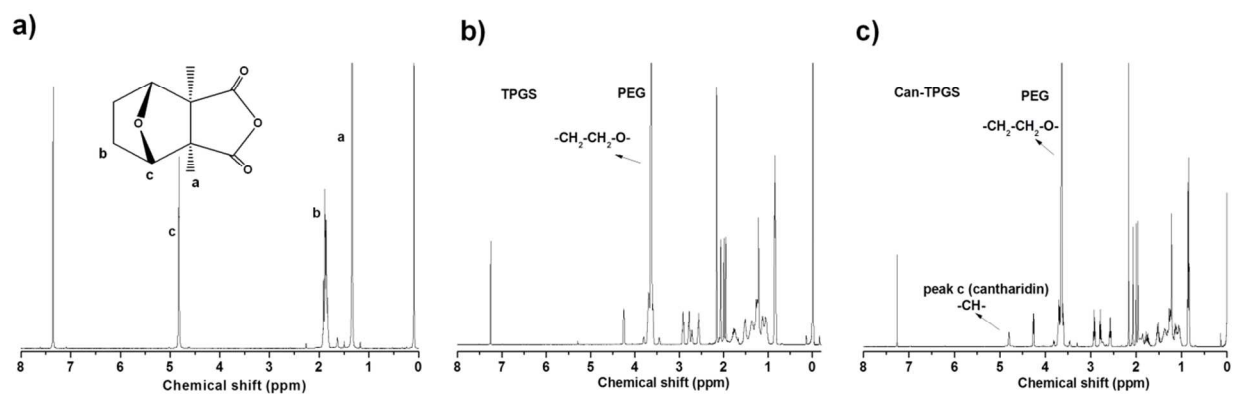


Figure 1. ¹H NMR spectra of cantharidin (a), TPGS (b) and Can-TPGS conjugate (c)

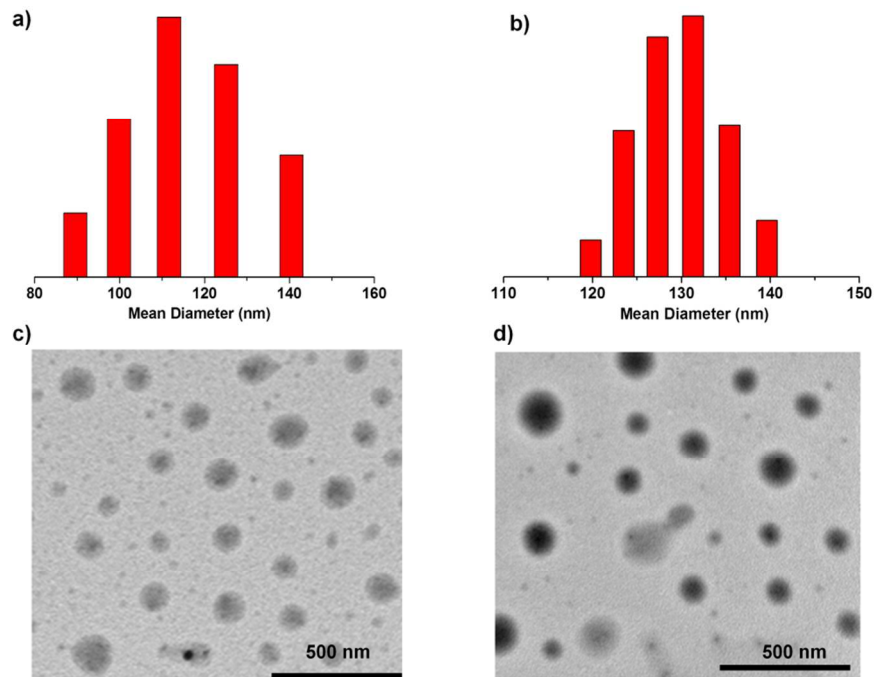


Figure 2. Characterization of cantharidin loaded nanoparticles Can-NPs (a,c) and folate targeting nanoparticles FA-Can-NPs (b,d) by DLS (a,b) and TEM (c,d). Can-NPs showed a mean diameter of 114.7 nm with a polydispersity index of 0.104 by DLS (a) and a mean diameter of 102.5 nm by TEM (c). Similarly, FA-Can-NPs showed a mean diameter of 130.4 nm with a polydispersity index of 0.216 by DLS (b) and a mean diameter of 110.7 nm by TEM (d).

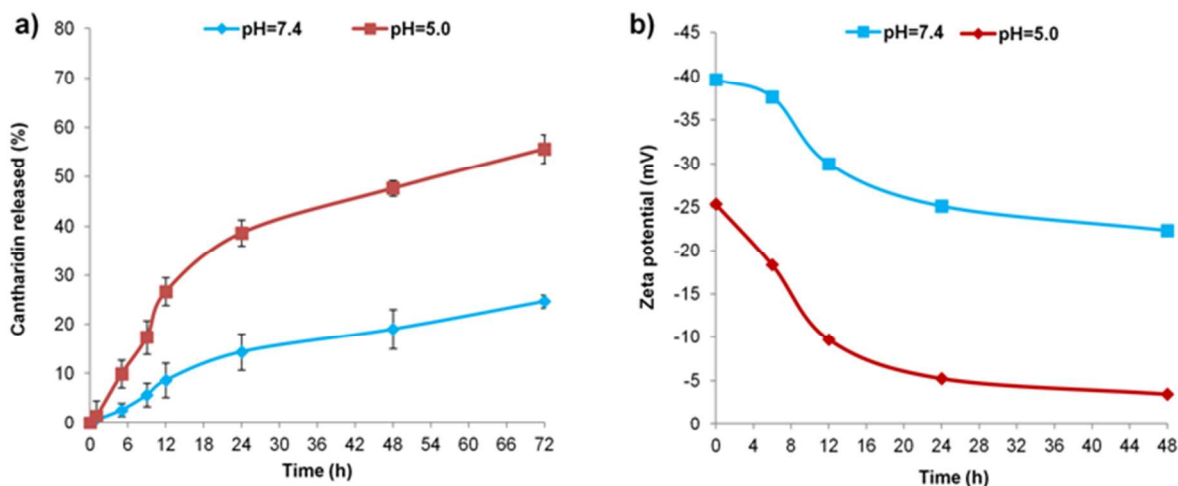


Figure 3. Representative drug release of cantharidin from Can-NPs studied by ^1H NMR at pH5.0 and pH7.4. Experimental details were shown in the text. Data were shown as mean value \pm standard deviation ($n=3$)(a). To give an insight into the nanoparticle change, the zeta potential of the nanoparticles were monitored during this process and the results were listed in (b).

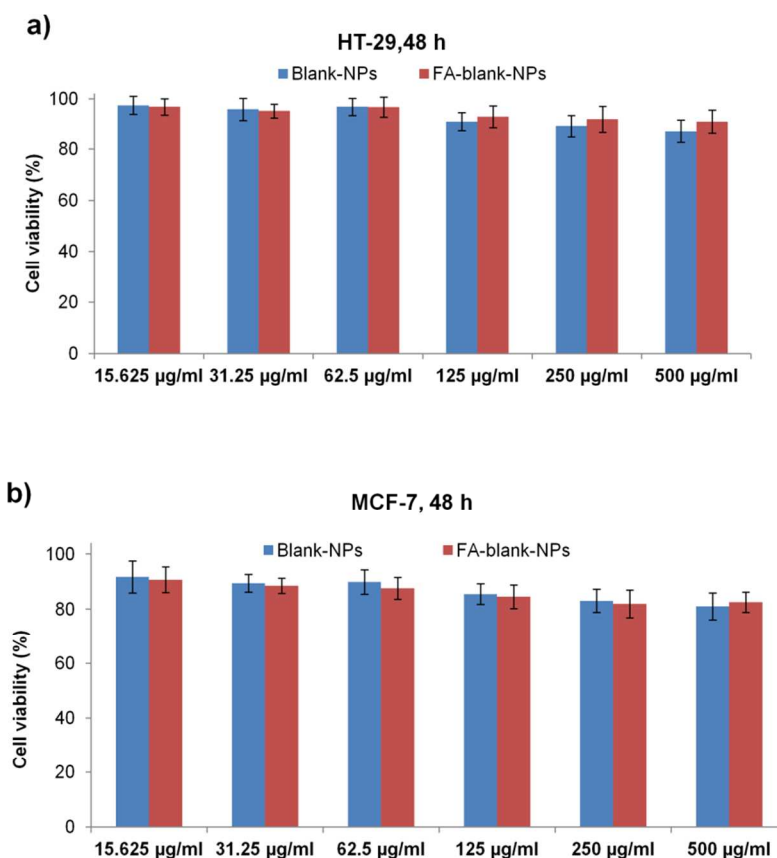


Figure 4. *In vitro* cytotoxicity of TPGS NPs and FA-TPGS NPs on HT-29 (a) and breast cancer MCF-7 (b) cells at 48 h (b). Data were shown as mean value \pm standard deviation ($n=4$).

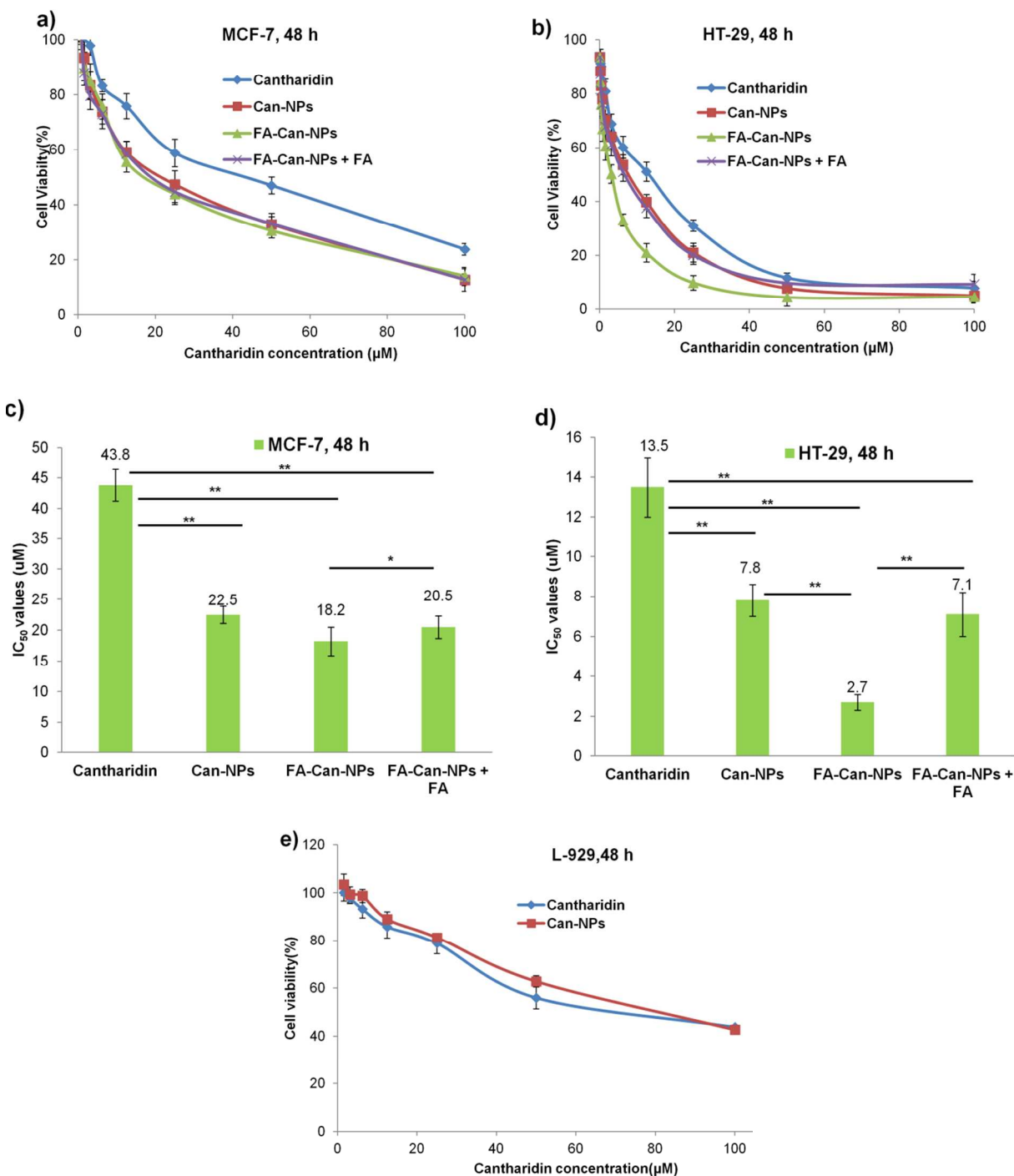


Figure 5. Representative *In vitro* cytotoxicity of cantharidin loaded nanoparticles Can-NPs and folate targeting nanoparticles with cantharidin (FA-Can-NPs) on Breast cells (a) and HT-29 cells (b) at 48 h and representative cytotoxicity of FA-Can-NPs via blocking the folate receptor by pre-incubating the cells with 2 mM folate for 1 h. The IC₅₀ values of cantharidin, Can-NPs, FA-Can-NPs and FA-Can-NPs blocked by free 2 mM FA on breast cancer MCF-7 (c) and HT-29 cells (d) at 48 h were collected. Data were shown as mean value \pm standard deviation (n=3). *** indicates $p < 0.001$, ** indicates $p < 0.01$. To further show the preference to kill the cancer cells, L-929 cells were treated with cantharidin and Can-NPs, MTT assay was performed (e).

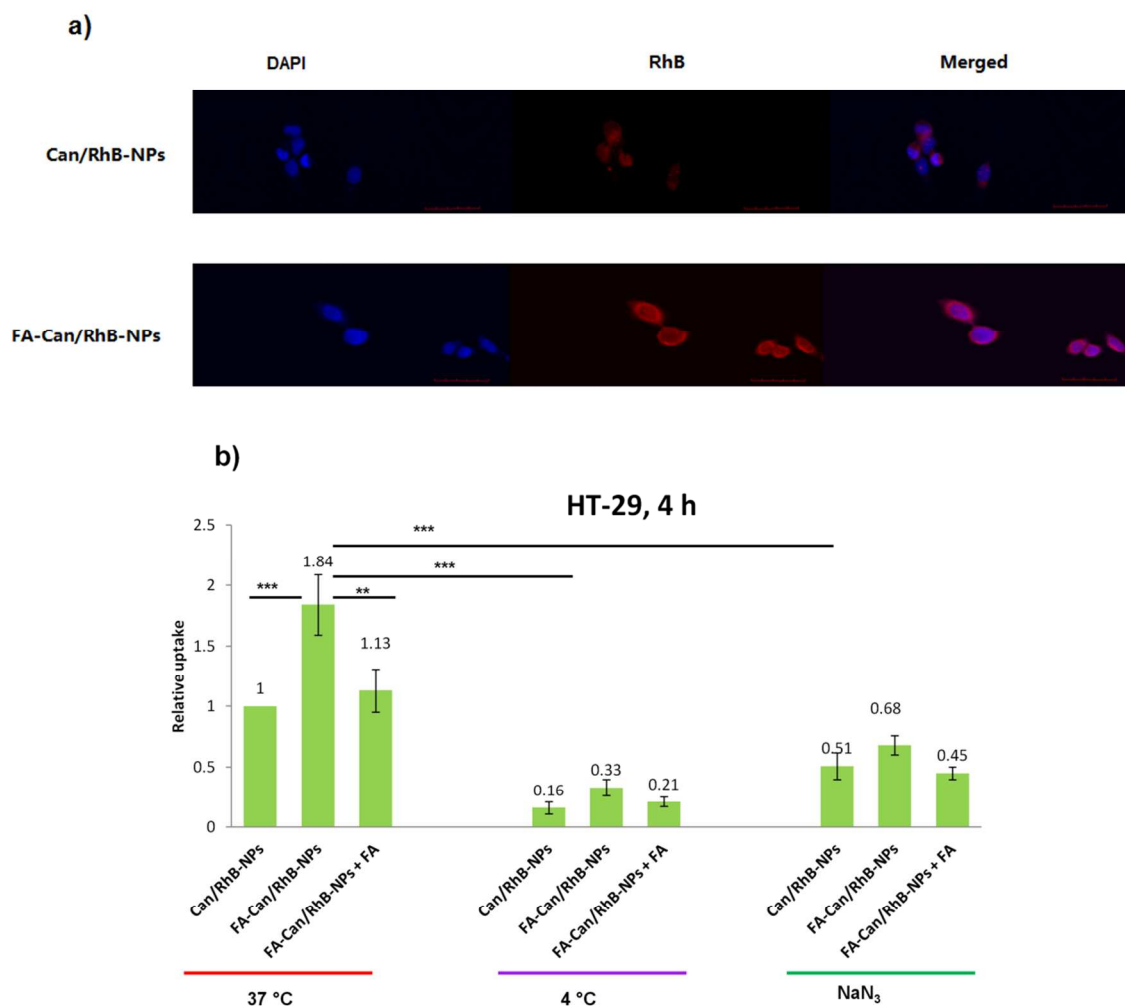


Figure 6 Intracellular uptakes of Can-NPs by HT-29 cancer cells. Representative confocal laser scanning images of Can/RhB-NPs and FA-Can/RhB-NPs with an equal RhB concentration of 2 $\mu\text{g}/\text{ml}$ at 1 h (a). After treatment of Can/RhB-NPs and FA-Can/RhB-NPs for 1 h, cells were thoroughly washed and fixed by with 4% formaldehyde. Cell nucleus was stained by DAPI (blue fluorescence) and then observed using confocal laser scanning microscope (CLSM, Olympus FV1000). The red fluorescence comes from RhB. The scale bar is 40 μm . The relative uptake study of Can-NPs, FA-Can-NPs and FA-Can-NPs blocked by 2 mM FA at 4 h via flow cytometry was shown in (b). Cells were treated with the drug cantharidin loaded micelles at 1 μM . RhB was 5 $\mu\text{g}/\text{ml}$. Results were shown as relative to Can-NPs at 37 °C for 4 h. Data were shown as mean value \pm standard deviation ($n=3$).). *** indicates $p<0.001$, ** indicates $p<0.01$.

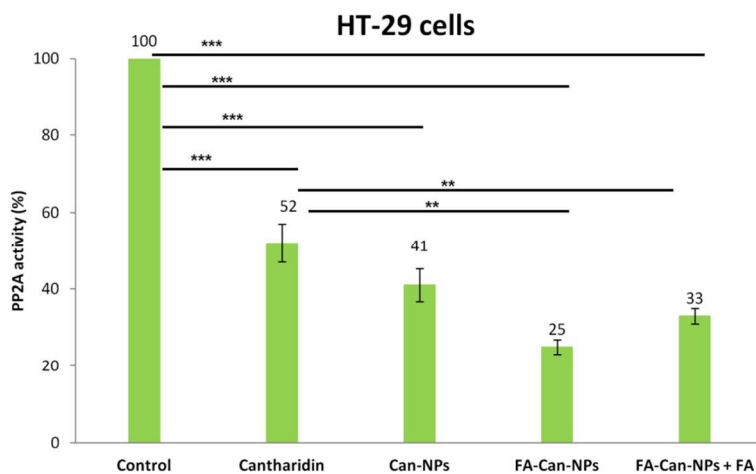


Figure 7. The PP2A activity of HT-29 cells treated with cantharidin, Can-NPs, FA-Can-NPs and FA-Can-NPs blocked by 2 mM FA. The non-treated cells were set as control. Data were shown as mean value \pm standard deviation ($n=3$).*** indicates $p<0.001$, ** indicates $p<0.01$.

Table 1. Physical parameters of the nanoparticles prepared

Code	DLS (nm)	PDI	Zeta Potential(mV)
TPGS NPs	65.7 ± 2.5	0.125	-22.1 ± 1.5
FA-TPGS NPs	72.4 ± 1.9	0.135	-29.2 ± 3.1
Can-NPs	114.7 ± 1.2	0.104	-35.6 ± 2.4
FA-Can-NPs	130.4 ± 3.2	0.216	- 28.4 ± 3.5

